Received: 19 July 2017 | Revised: 10 August 2018 | Accepted: 16 September 2018

DOI: 10.1111/bre.12317

ORIGINAL ARTICLE

WILEY Basin Research IAS EAGE

# New insights on measured and calculated vitrinite reflectance

**Tim Matava**[1] | **Veit Matt**[2] | **Jack Flannery**[3]

[1]GGIM Inc., Houston, Texas

[2]ConocoPhillips Company, Houston, Texas

[3]Houston, Texas

**Correspondence**
Tim Matava, GGIM Inc., Houston, TX.
Email: tmatava@sbcglobal.net

**Abstract**

Measurement of dispersed vitrinite reflectance in organic sediments is one of the few regional data sets used for placing bounds on the thermal history of a sedimentary basin. Reflectance data are important when access to complementary information such as high-quality seismic data is unavailable to place bounds on subsidence history and in locations where uplift is an important part of the basin history. Attributes which make vitrinite reflectance measurements a useful data set are the relative ease of making the measurement, and the availability of archived well cores and cuttings in state, provincial, and federal facilities. In order to fully utilize vitrinite data for estimating the temperature history in a basin, physically based methods are required to calibrate an equivalent reflectance from a modelled temperature history with measured data. The most common method for calculating a numerical vitrinite reflectance from temperature history is the EASY%$R_o$ method which we show systematically underestimates measured data. We present a new calculated reflectance model and an adjustment to EASY%$R_o$ which makes the correlation between measured vitrinite values and calculated vitrinite values a physical relationship and more useful for constraining thermal models. We then show that calibrating the thermal history to vitrinite on a constant age date surface (e.g., top Cretaceous) instead of calibrating the thermal history in depth removes the heating rate component from the reflectance calculation and makes thermal history calibration easier to understand and more directly related to heat flow. Finally, we use bounds on the vitrinite–temperature relationships on a constant age date surface to show that significant uncertainty exists in the vitrinite data reported in most data sets.

## 1 | INTRODUCTION

Time and temperature have long been understood as fundamental controls on the transformation of load-bearing organic matter to liquid hydrocarbons, and a variety of visual methods have been developed to estimate time–temperature effects with information obtained from well cuttings and cores. Some of these methods include a Thermal Alteration Index on pollen and spores, the use of microfossils to form various indices such as ostracod, conodonts, and foraminifera alteration indices (Fleisher & Lane, 1999; Rejebian, Harris, & Huebner, 1987). Visual analysis of the reflectance of vitrinite in core and cutting samples is currently the most commonly used method for estimating the effect of increases in temperature through time on the thermal maturity of organic material. It is generally accepted that vitrinite reflectance improves on earlier developed visual methods (Fleisher & Lane, 1999; Hackley & Cardott, 2016). Well-established methods are available for measuring vitrinite reflectance of coals (e.g., ASTM D7708) and these methods have been adapted for measuring the reflectance of vitrinite dispersed in sedimentary rocks (Hackley & Cardott, 2016; Hackley et al., 2015).

Various groups and associations, including the International Committee for Coal and Organic Petrology (ICCP), the Society of Organic Petrology (SOP), and the American Association of Petroleum Geologists (AAPG), have further developed these methods to better apply vitrinite measurements for oil and gas exploration. Even with these efforts to introduce standards, round robin results show that a wide range of measurements are reported with standard deviations typically of 0.1–0.2 for a single set of slides analysed by different operators utilizing different equipment (Hackley et al., 2015).

Vitrinite is composed of a narrow range of relatively easily identifiable macerals and has become the standard measure for organic maturity (Mukhopadhyay, 2014). The narrow range of macerals leads to a small range of physical and chemical kinetic properties and a consistent response to increasing temperature through time regardless of the geologic setting. Well-established vitrinite reflectance values with relatively small ranges have been developed that correspond to the various stages of hydrocarbon generation from source rocks containing kerogen (e.g., immature, early mature, mature, and overmature) by Poole and Claypool (1984); Jarvie, Hill, and Pollastro (2005) and they apply to any geologic basin. Additionally, samples are easy to obtain and modest levels of laboratory equipment are required to prepare and analyse these samples. These attributes of vitrinite have resulted in large public domain reflectance databases archived at state, provincial, and federal facilities.

Multidimensional numerical basin simulation tools (basin simulators) were originally developed to forward model the temperature history in a basin in order to estimate the potential and timing for hydrocarbon generation from source rocks. Because the timing of generation depends on the mineral matrix, type of organic matter and kerogen, and the temperature and heating rate, vitrinite reflectance is useful for separating the compositional control on generation from the thermal control on generation. Two numerical algorithms to calculate the vitrinite reflectance from temperature histories are VITRIMAT (Burnham & Sweeney, 1989) and a simpler version of the same algorithm called EASY%$R_o$ (Sweeney & Burnham, 1990). The EASY%$R_o$ algorithm is incorporated in most simulators currently available; the VITRIMAT tool is no longer generally available and has never been incorporated in any commercial basin simulator.

The utility of vitrinite reflectance measurements and EASY%$R_o$ in the oil and gas exploration industry is clear. However, measurement of vitrinite reflectance on dispersed organic matter is not without uncertainty. Sources of uncertainty are reviewed in detail by Hackley and Cardott (2016) and include caving, and correct identification of macerals. Hackley et al. (2015) have shown that different operators viewing the same slide may not always choose the same macerals for measurement. Additionally, reflectance may vary within a particular vitrinite maceral (Goodarzi & Murchison, 1973) and reflectance is anisotropic (Malinconico, 2000). Local generation or the presence of migrated hydrocarbons may suppress the maturity of vitrinite (Fang & Jianyu, 1992; Price & Barker, 1985). Complementary methods have been developed to address suppression in early mature sediments (Thompson-Rizer & Woods, 1987) including fluorescence alteration of multiple macerals (FAMM) which suggests that suppression can be up to approximately 20% (Kalkreuth et al., 2004; Veld, Wilkins, Xianming, & Buckingham, 1997; Wilkins, Sherwood, Faiz, Teerman, & Buckingham, 1997; Wilkins et al., 1992). Sample slides previously prepared for vitrinite reflectance measurements may require repolishing to yield consistent results because of oxidation of the organic material on the slide surface. Finally, interpretation and application of these data are made more difficult because the agencies responsible for the databases require operators to report only a single value without any supplementary information to help qualify the reported data.

Uplift and the associated erosion and cooling are interpreted from changes in the slope of vitrinite data with depth (Dow, 1977; Katz, Pheifer, & Schunk, 1988; Wood, 1988). Dow's method, essentially a continuity condition on vitrinite changes with temperature, shows how to estimate erosion from discontinuities in vitrinite profiles that are associated with reheating after an uplift event during reburial. Dow's continuity condition means that vitrinite must be reheated to a temperature greater than the previous maximum temperature for the reaction to proceed.

Robust calibration of calculated vitrinite reflectance to measured data is required to relate vitrinite data to

### Highlights

- This paper pertains to the use of measured vitrinite reflectance as a tool to constrain the thermal history of sedimentary basins.
- We show that an often used model to calculate reflectance systematically underestimates measured reflectance of a data set used in the original calibration and we propose two methods to remedy this result.
- These results indicate that measured and calculated reflectances need to be compared to avoid bias in using these data to constrain thermal history of basins.
- Finally, we show that calibration basin models on chronostratigraphic surfaces removes the time variable from the reflectance calculation making the calibration dependent only on the maximum temperature.

temperature history. Sweeney and Burnham (1990) compared EASY%$R_o$ with measured reflectance data at a maximum temperature and noted a favourable relationship. However, they did not compare calculated values with measured data directly to determine the predictive ability of their model. We start with a direct comparison of measured reflectance data and calculated reflectance values used in EASY%$R_o$ (Sweeney & Burnham, 1990), but we limit our comparison to the burial diagenesis data set, Table 5.2 in Barker (1989), and do not consider applications to geothermal systems or contact metamorphism. In addition to a direct comparison of EASY%$R_o$, we also use the data set to propose a new vitrinite reflectance model which we refer to as the BDW model after contribution to this technology by Barker, Dow, and Wood. Next, in a series of applications, we consider the use of vitrinite reflectance measurements to constrain the thermal history. These results illustrate the difference between adjusting a thermal model to match measured vitrinite data and a physically bounded thermal model that constrains the thermal history. Finally, we show that the wide range of vitrinite data available in basins has significant uncertainty suggesting that care must be used when vitrinite is employed to constrain thermal models to changes in temperature through time.

We use public data sets available from government agencies and refer to reported vitrinite reflectance data as $R_m$ and reflectance calculated from temperature and heating rate histories as $R_c$, with an appropriate superscript. Our definition of measured vitrinite reflectance data, $R_m$, is limited because these public data sets contain both individual measurements and mean values of distributions, and we do not suppose that we can always distinguish between the two. Our definitions for calculated vitrinite values from temperature histories may be the same as others have reported as vitrinite reflectance equivalent (VRE). However, VRE is sometimes used to refer to values derived from other measurements (e.g., $T_{max}$) or other thermal alteration measures (e.g., TAI of conodonts, pollens, and spores).

## 2 | CALCULATING VITRINITE REFLECTANCE

A comparison of measured and calculated reflectance values using thermal histories is a basic part of constraining thermal models to better understand the timing of hydrocarbon generation. Of fundamental importance is how well a vitrinite numerical model is calibrated to measured data. Only the model results are discussed in this section: the mathematical development of the models, and methods for calculating coefficients from the data are provided in the Appendix A. The appendix includes a section on the range of uncertainty in vitrinite calculations due uncertainty in temperature. The

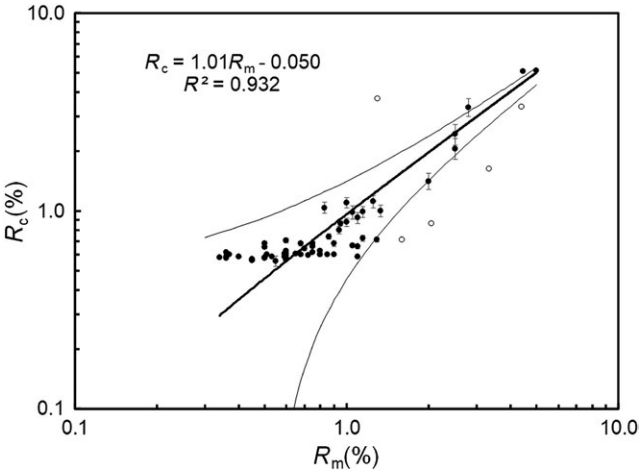


**FIGURE 1** Measured vitrinite reflectance and calculated vitrinite reflectance using data from Table 5.2 in Barker (1989) and reproduced in Table 1. This model, which we refer to as the BDW model, is a bulk model with coefficients derived from these data. Error bands are derived from the standard error of the estimate which is 0.482. Each solid data point is included in the correlation and has an error bar which corresponds to the uncertainty in calculated reflectance due to a 2.5% uncertainty in absolute maximum or present day temperature (±9.3°C at 100°C). Details and calculations of how temperature uncertainty affects the vitrinite reflectance calculation are presented in the appendix. Open circles are not included in the correlation between measured and calculated reflectance and are excluded from all calculations of coefficients

appendix also contains Table 5.2 from Barker (1989) with columns appended to show calculated reflectance values and ranges in these calculated values due to uncertainties in present day or maximum temperature.

A direct comparison of measured and calculated vitrinite reflectance is shown in Figures 1 and 2. Figure 1 shows measured reflectance ($R_m$) values and calculated reflectance ($R_c$) values using coefficients derived from the Barker (1989) data set (the BDW model). Figure 2 shows measured reflectance data and calculated EASY%$R_o$ reflectance values. Both figures contain error bands that are calculated from the standard error of the least square fit to the data. In Figure 1, there are five data points with open circles outside the error bands which are included the standard error of the estimate but not in the least squares fit. Error bars on each data point are estimates of the uncertainty in $R_c$ due to a 2.5% uncertainty in absolute present day or maximum temperature (±9.3°C at 100°C). Estimates of uncertainty in the $R_m$ data are not available because distributions of individual measurements are not reported.

Figures 1 and 2 both show a reasonable linear fit between $R_m$ and $R_c$; however, there are important distinctions between models. The range of the models are 0.56% < $R_c^{BDW}$ <5.2% and 0.20% < EASY%$R_o$ <4.7%. The BDW model has significant uncertainty at the lower limit of measured reflectance

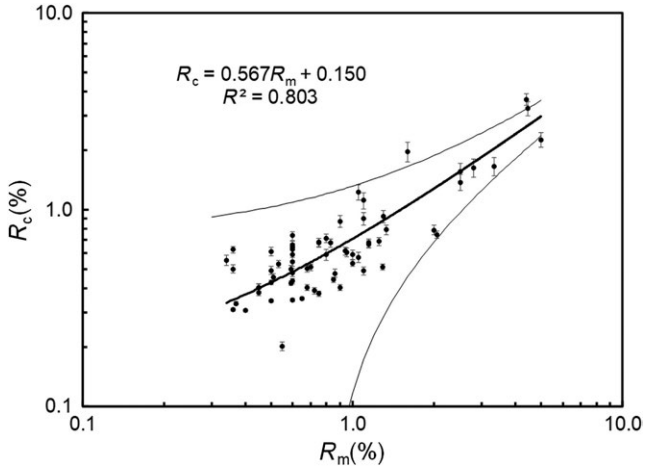


**FIGURE 2** Measured vitrinite reflectance and EASY%$R_o$ using Sweeney and Burnham (1990). Measured data are from Table 5.2 in Barker (1989) as are the functional heating time and temperature. The least squares fit to these data shows that the EASY%$R_o$ model systematically underestimates the measured reflectance by more than 40%. The implications of the underestimate in the calculation is discussed in the text. Error bands are derived from the standard error of the estimate which is 0.600. Error bars are based on maximum or present day temperature uncertainty similar to the BDW model (Figure 1)

that is not apparent in the EASY%$R_o$ model. However, the BDW model matches measured reflectance better than the EASY%$R_o$ model when reflectance values are greater than 0.75%. An important difference in the two models is that the BDW model is a bulk model derived from the data in Table 5.2 Barker (1989), so the uncertainty at low reflectance values directly affects the correlation. In contrast, the EASY%$R_o$ model is a chemical model and it is the result of a series of reactions occurring during thermal diagenesis of organic matter. Since EASY%$R_o$ pre-supposes a model for changes in vitrinite, it better addresses the uncertainty of the low measured reflectance. Another important difference between the two models is that $\frac{dR_c}{dR_m} \approx 1$ in the BDW model and is $\approx 0.56$ in the EASY%$R_o$ model.

The slope of calculated to measured reflectance curve is not 1 in the EASY%$R_o$ model which has significant implications on thermal history used in the basin simulator to calibrate the model. Because $R_m$ changes much faster than $R_c$ in the EASY%$R_o$ model, the heat flow must be adjusted higher for $R_c$ to match $R_m$. Furthermore, since a thermal model must also match bottom hole temperature (BHT) data, high heat flows required to match the measured vitrinite reflectance are decreased to match the measured temperature data. These heat flow adjustments are not required with the BDW model. This aspect of the EASY%$R_o$ model was implied by Sweeney and Burnham (1990) when they adjusted temperature gradients to fit data in their examples, but the physical implication of these changes was not addressed.

Errors in maturity estimates have an asymmetric impact on estimates of prospectivity. Exploring in a basin when the source rock maturity is underestimated leads to an outcome where the hydrocarbon product may contain more gas and less liquid than estimated. Exploring in a basin where the source maturity is overestimated and the source rock is immature leads to an outcome where no hydrocarbon product has been generated and all exploration efforts are misdirected. The heat flow adjustments required to match $R_c$ to $R_m$ with EASY%$R_o$ generally imply that the calculated source rock maturity is higher than the actual maturity of the source rock. Such a result passes the geologic risk of the opportunity on to the model used to evaluate the opportunity.

A post-processor adjustment to EASY%$R_o$-calculated reflectance values is possible to improve the relation between measured and calculated values. This adjustment is a linear transformation of the data and does not affect the statistics of the curve fit. It has the form

$$R_c^{adj}(\%) = 1.7652R_c(\%) - 0.265 \quad (1)$$

In summary, two methods are presented for calculating vitrinite reflectance from temperature changes through time. The EASY%$R_o$ method is based on a chemical model with multiple reactions occurring during heating; however, the calculated reflectance is significantly less than the measured reflectance. The BDW model is a bulk model with coefficients derived from measured data. The BDW model lacks the low range of the EASY%$R_o$ model but matches measurements better. The BDW model lacks the chemical foundation of the EASY%$R_o$ model.

## 3 | APPLICATION

Several examples are presented to illustrate the differences between EASY%$R_o$ and BDW models. First, two examples of vitrinite profiles from wells on the coast of the Gulf of Mexico illustrate the use of vitrinite to constrain heat flow in wells. Next, two examples are shown from the Denver–Julesburg (DJ) Basin one of which illustrates the utility of calibrating vitrinite models on a regional chronostratigraphic surface.

Examples of the two vitrinite reflectance models applied to well data are shown in Figures 3 and 4. These data are from Dow (1977) and include a large section of Miocene age sediments in onshore wells in the Gulf of Mexico area. In these two examples, the objective is to fit vitrinite data in a way that provides information on the heat flow history. In both examples, the burial rate is taken as a constant, temperatures are assumed steady state, and the bulk thermal conductivity is 1.5 $W\,m^{-1}\,K^{-1}$ which is

**TABLE 1** Table 5.2 from Barker (1989) filtered for measured reflectance. Columns appended to this table are the calculated reflectance values from the BDW and EASY%$R_o$ models using the temperature and heating duration. Calculated vitrinite values consist of two columns for each model. The first column is the calculated value and the second column is the fractional error ($\frac{\delta R_c}{R_c}$) due to a 2.5% uncertainty in measured temperature (e.g., ±9.3°C at 100°C). At the end of this table are five rows of data in bold. These data are not used in the curve fits for the BDW method, and in Figures 1, A1 and A2 these data are identified with open circles. In these calculations, the initial temperature is taken to be 10°C and the heating rate is constant during the duration of heating

| | | | | | $R_c^{BDW}$ | | EASY%$R_o$ | |
|---|---|---|---|---|---|---|---|---|
| Temperature (°C) | Heating duration (Ma) | Measured reflectance (%) | Reaction remaining fraction | Ln (K) ($s^{-1}$) | (%) | Error | (%) | Error |
| 95 | 0.32 | 0.45 | 0.98 | −33.8 | 0.56 | 4.61E-04 | 0.40 | 4.19E-02 |
| 95 | 0.63 | 0.45 | 0.98 | −34.5 | 0.56 | 9.20E-04 | 0.40 | 4.33E-02 |
| 164 | 0.19 | 0.60 | 0.89 | −31.6 | 0.57 | 2.10E-03 | 0.74 | 5.13E-02 |
| 80 | 3.17 | 0.45 | 0.98 | −36.1 | 0.57 | 2.59E-03 | 0.38 | 3.67E-02 |
| 143 | 0.63 | 0.60 | 0.89 | −32.8 | 0.57 | 4.05E-03 | 0.66 | 4.53E-02 |
| 65 | 6.34 | 0.50 | 0.95 | −35.9 | 0.58 | 2.75E-03 | 0.34 | 2.11E-02 |
| 52 | 9.51 | 0.36 | 0.99 | −37.9 | 0.58 | 2.22E-03 | 0.31 | 1.49E-02 |
| 137 | 0.95 | 0.60 | 0.89 | −33.2 | 0.58 | 5.13E-03 | 0.65 | 4.01E-02 |
| 131 | 1.27 | 0.60 | 0.89 | −33.5 | 0.58 | 5.75E-03 | 0.63 | 4.78E-02 |
| 105 | 2.54 | 0.50 | 0.95 | −35.0 | 0.58 | 5.12E-03 | 0.49 | 4.92E-02 |
| 118 | 1.90 | 0.34 | 0.99 | −36.3 | 0.58 | 5.83E-03 | 0.55 | 5.69E-02 |
| 105 | 2.85 | 0.59 | 0.90 | −34.4 | 0.59 | 5.74E-03 | 0.50 | 4.75E-02 |
| 112 | 2.54 | 0.53 | 0.93 | −34.6 | 0.59 | 6.41E-03 | 0.53 | 4.31E-02 |
| 48 | 15.9 | 0.40 | 0.99 | −37.9 | 0.59 | 2.98E-03 | 0.31 | 1.22E-02 |
| 105 | 3.17 | 0.36 | 0.99 | −36.8 | 0.59 | 6.36E-03 | 0.50 | 4.58E-02 |
| 128 | 3.17 | 0.36 | 0.99 | −36.8 | 0.62 | 1.28E-02 | 0.63 | 3.77E-02 |
| 113 | 3.17 | 0.60 | 0.89 | −34.4 | 0.60 | 8.22E-03 | 0.54 | 5.03E-02 |
| 75 | 9.51 | 0.72 | 0.81 | −34.9 | 0.60 | 6.22E-03 | 0.39 | 3.72E-02 |
| 90 | 6.34 | 0.85 | 0.73 | −34.1 | 0.60 | 7.44E-03 | 0.44 | 3.33E-02 |
| 120 | 2.85 | 0.80 | 0.77 | −33.5 | 0.60 | 9.19E-03 | 0.59 | 6.34E-02 |
| 78 | 9.51 | 0.68 | 0.84 | −35.1 | 0.60 | 7.01E-03 | 0.40 | 3.68E-02 |
| 78 | 9.51 | 0.90 | 0.71 | −34.4 | 0.60 | 7.01E-03 | 0.40 | 3.68E-02 |
| 55 | 19.0 | 0.37 | 0.99 | −37.9 | 0.60 | 5.05E-03 | 0.33 | 2.23E-02 |
| 93 | 6.34 | 0.51 | 0.94 | −35.7 | 0.60 | 8.28E-03 | 0.46 | 4.27E-02 |
| 63 | 15.9 | 0.65 | 0.86 | −35.2 | 0.61 | 6.13E-03 | 0.35 | 1.72E-02 |
| 97 | 6.34 | 0.60 | 0.89 | −35.1 | 0.61 | 9.51E-03 | 0.48 | 4.89E-02 |
| 83 | 9.51 | 0.59 | 0.90 | −35.6 | 0.61 | 8.49E-03 | 0.42 | 2.67E-02 |
| 60 | 19.0 | 0.60 | 0.89 | −35.5 | 0.61 | 6.39E-03 | 0.35 | 1.72E-02 |

*(Continues)*

**TABLE 1** (Continued)

| Temperature (°C) | Heating duration (Ma) | Measured reflectance (%) | Reaction remaining fraction | Ln (K) ($s^{-1}$) | $R_c^{BDW}$ (%) | $R_c^{BDW}$ Error | EASY%$R_o$ (%) | EASY%$R_o$ Error |
|---|---|---|---|---|---|---|---|---|
| 135 | 2.85 | 0.75 | 0.80 | −33.6 | 0.62 | 1.41E-02 | 0.68 | 4.96E-02 |
| 140 | 2.85 | 0.80 | 0.77 | −33.5 | 0.63 | 1.61E-02 | 0.71 | 5.11E-02 |
| 84 | 12.7 | 0.60 | 0.89 | −35.8 | 0.63 | 1.16E-02 | 0.43 | 2.76E-02 |
| 100 | 9.51 | 0.70 | 0.83 | −35.0 | 0.64 | 1.54E-02 | 0.51 | 3.88E-02 |
| 80 | 19.0 | 0.50 | 0.95 | −36.3 | 0.65 | 1.46E-02 | 0.43 | 2.49E-02 |
| 183 | 1.59 | 1.10 | 0.59 | −32.1 | 0.66 | 2.53E-02 | 1.12 | 9.44E-02 |
| 65 | 31.7 | 0.75 | 0.80 | −34.8 | 0.66 | 1.29E-02 | 0.37 | 2.88E-02 |
| 110 | 9.51 | 1.05 | 0.62 | −33.9 | 0.67 | 2.11E-02 | 0.57 | 6.05E-02 |
| 130 | 6.34 | 0.75 | 0.80 | −30.8 | 0.68 | 2.58E-02 | 0.68 | 4.94E-02 |
| 160 | 3.17 | 0.90 | 0.71 | −33.3 | 0.68 | 2.88E-02 | 0.87 | 7.10E-02 |
| 95 | 15.9 | 0.68 | 0.84 | −35.1 | 0.68 | 2.09E-02 | 0.50 | 4.09E-02 |
| 115 | 9.51 | 0.50 | 0.95 | −36.5 | 0.69 | 2.45E-02 | 0.61 | 5.23E-02 |
| 121 | 9.51 | 0.60 | 0.89 | −35.5 | 0.71 | 2.90E-02 | 0.65 | 3.56E-02 |
| 110 | 12.7 | 0.60 | 0.89 | −35.5 | 0.71 | 2.73E-02 | 0.59 | 6.03E-02 |
| 96 | 19.0 | 1.29 | 0.47 | −33.6 | 0.71 | 2.54E-02 | 0.51 | 3.66E-02 |
| 125 | 9.51 | 1.15 | 0.56 | −33.9 | 0.73 | 3.23E-02 | 0.67 | 4.39E-02 |
| 87 | 28.5 | 0.86 | 0.73 | −34.5 | 0.74 | 2.68E-02 | 0.48 | 4.53E-02 |
| 111 | 19.0 | 0.94 | 0.68 | −34.3 | 0.80 | 3.97E-02 | 0.62 | 4.83E-02 |
| 105 | 28.5 | 1.00 | 0.65 | −34.2 | 0.88 | 4.64E-02 | 0.59 | 5.82E-02 |
| 155 | 9.51 | 1.10 | 0.59 | −34.0 | 0.93 | 6.42E-02 | 0.90 | 7.25E-02 |
| 180 | 6.34 | 1.05 | 0.62 | −33.7 | 0.99 | 7.50E-02 | 1.23 | 9.18E-02 |
| 120 | 25.4 | 1.15 | 0.56 | −34.8 | 0.99 | 6.18E-02 | 0.68 | 4.60E-02 |
| 140 | 15.9 | 1.33 | 0.44 | −33.5 | 1.00 | 6.85E-02 | 0.79 | 5.79E-02 |
| 119 | 28.5 | 0.83 | 0.75 | −34.5 | 1.04 | 6.54E-02 | 0.68 | 4.54E-02 |
| 93 | 63.4 | 1.00 | 0.65 | −34.2 | 1.10 | 5.89E-02 | 0.54 | 4.08E-02 |
| 120 | 31.7 | 1.25 | 0.50 | −33.7 | 1.12 | 7.14E-02 | 0.69 | 4.79E-02 |
| 135 | 31.7 | 2.00 | 0.17 | −32.8 | 1.41 | 9.29E-02 | 0.79 | 5.58E-02 |
| 180 | 19.0 | 2.50 | 0.10 | −32.5 | 2.07 | 1.20E-01 | 1.38 | 9.45E-02 |
| 190 | 19.0 | 2.50 | 0.10 | −32.5 | 2.44 | 1.21E-01 | 1.56 | 1.02E-01 |
| 190 | 28.5 | 2.80 | 0.07 | −32.4 | 3.34 | 1.02E-01 | 1.63 | 1.08E-01 |

*(Continues)*

**TABLE 1** (Continued)

| Temperature (°C) | Heating duration (Ma) | Measured reflectance (%) | Reaction remaining fraction | Ln (K) ($s^{-1}$) | $R_c^{BDW}$ (%) | Error | EASY%$R_o$ (%) | Error |
|---|---|---|---|---|---|---|---|---|
| 252 | 28.5 | 4.45 | 0.01 | −31.8 | 5.10 | 1.00E-02 | 3.28 | 8.03E-02 |
| 210 | 63.4 | 5.00 | 0.01 | −31.8 | 5.12 | 6.90E-03 | 2.27 | 8.73E-02 |
| 103 | 9.51 | 1.10 | 0.59 | −34.0 | 0.59 | 5.95E-03 | 0.49 | 4.94E-02 |
| 58 | 31.7 | 0.55 | 0.92 | −35.8 | 0.56 | 4.00E-02 | 0.20 | 5.11E-02 |
| 108 | 25.4 | 0.95 | 0.68 | −43.3 | 0.86 | 4.00E-02 | 0.61 | 5.11E-02 |
| **141** | **95.13** | **1.30** | **0.47** | **−35.6** | **3.68** | **8.05E-2** | **0.93** | **7.50E-2** |
| **233** | **0.95** | **1.60** | **0.29** | **−30.8** | **0.72** | **3.95E-2** | **1.97** | **1.13E-1** |
| **135** | **12.68** | **2.05** | **0.17** | **−32.8** | **0.86** | **5.24E-2** | **0.75** | **4.10E-2** |
| **200** | **9.51** | **3.35** | **0.04** | **−32.2** | **1.63** | **1.18E-1** | **1.66** | **1.10E-1** |
| **279** | **6.34** | **4.40** | **0.01** | **−31.5** | **3.37** | **1.10E-1** | **3.64** | **7.12E-2** |

the upper limit of a shale sediment (Blackwell & Steele, 1989). No BHT data is available for these wells. Inset into each figure is the heat flow history used to generate the vitrinite profile.

Figures 3 and 4 show that the EASY%$R_o$ calculation fits the data well over the vertical profile; however, the heat flow histories required to match the profile are not constant. High heat flows are required early to increase the time deeper sediments are exposed to higher temperatures. The heat flow is decreased later in the model in order to match the shallow portion of the well. In contrast to the EASY%$R_o$ model, the profiles using the BDW model are not useful for the shallow portion of the well where the reflectance is small (<0.56%), but for the rest of the profile, a simple heat flow model is required to match the data. Reflectance values less than 0.56% are the early phase of vitrinite transformation which is near the start of the oil window (Jarvie et al., 2005; Poole & Claypool, 1984). The uncertainty of the EASY%$R_o$ model at these low vitrinite ranges is large.

The EASY%$R_o$ method requires a time variable heat flow to match a vitrinite profile over a significant vertical depth. Although this profile matches the data, the heat flow model is misleading since $\frac{dR_c}{dR_m} = 0.56$. This heat flow is misleading since these data are from the Gulf coast which is far from any interpreted location of the Cretaceous rift. Such a heat flow model may result in $R_c$ matching $R_m$, but it is non-physical because it is not based on a heat flow history consistent with a geologic model. Structural interpretations, such as rifting events, which affect the heat flow are not possible using the EASY%$R_o$ model. In contrast to the EASY%$R_o$ model, the BDW model does not fit the vitrinite profile over the entire range of data because the lower limit of applicability is $R_c < 0.56$, but the model is physical because the heat flow is consistent with structural interpretations.

In a second example from the Denver–Julesburg Basin, most of the measured vitrinite data are archived in government facilities and data from several operators are often mixed and do not extend over a significant portion of the well. Figure 5 is a plot of vitrinite with depth using public data from four closely spaced wells. In Figure 5, a wide range of vitrinite data is reported over a short vertical distance. Some of the data in Figure 5 appear to be individual measurements, possibly from a single prepared slide, while other data appear to be either single measurements or a single value reported from a suite of measured data. The spread of data over this short distance and the lack of supplementary information to qualify these data lead to maturity interpretations ranging from early to late oil maturity. A variety of circumstances can lead to this profile and the variation in data cannot necessarily be attributed to measurement error or caving in a well. For example, lithological changes or spatial changes in heat flow over small distances, such as may occur at a fault, may lead to

temperature changes which affect the measured reflectance. Because it is not possible to discern which data to use for interpretation and which data to discard all the reported data are considered valid.

Instead of calibrating to depth profiles of measured reflectance, Figures 3–5, we find it useful to calibrate basin models to vitrinite data on a chronostratigraphic surface. Equation A5 shows that the variables affecting $R_c$ may be reduced to temperature only when the calibrations are conducted on a constant age date surface. In an area with a simple heat flow model and no uplift (e.g., a continental margin or abyssal environment), interpolating vitrinite measurements to a chronostratigraphic surface transforms $R_c$ into a monotonic function of temperature. In areas with complex basement structure and heat flow, or in areas with uplift, Equation A5 is no longer strictly monotonic; however, the range of $R_c$ versus maximum temperature values is limited.

Applying extractions on a time surface in the Denver–Julesburg Basin show a comparison between maximum modelled temperature to $R_c$ (in this case EASY%$R_o$) and $R_m$, but the basin has experienced a significant amount of late uplift and erosion. Therefore, the maximum temperature is in part determined by the timing and magnitude of uplift. As before, the thermal model is calibrated to present day temperature with corrected BHT data and a physical model which uses a heat flow history determines the temperature through time. Figure 6 shows the maximum modelled temperature on the top of the Niobrara surface and $R_c$ as well as $R_m$ data. Vitrinite reflectance is used in the DJ Basin to constrain the heat flow and uplift history.

Figure 6 also shows measured vitrinite data and maximum modelled temperature averaged in 10°C windows starting at 40°C. For maximum temperatures between 70 and 130°C, the standard deviation of the vitrinite measurements in each 10°C window ranges from 0.1 to 0.2 which is similar to ranges reported by Hackley et al. (2015) in an extensive interlaboratory study. Even with this quality of vitrinite data, enough noise is present to support a number of interpretations. Averaging the data in temperature windows is an alternative to trying to identify a correct suite of individual measurements for interpretation.

Averaging the vitrinite data in temperature windows aids the interpretation of model results; however, it is not without significant implications. Averaging the data assumes each vitrinite measurement is equally as valid as any other measurement (Galton, 1907) and operator experience, or equipment quality cannot be used to weigh data for analysis. Additionally, data thought to be affected by systematic errors such as equipment malfunctions cannot be excluded from the analysis. While the averaging approach appears to

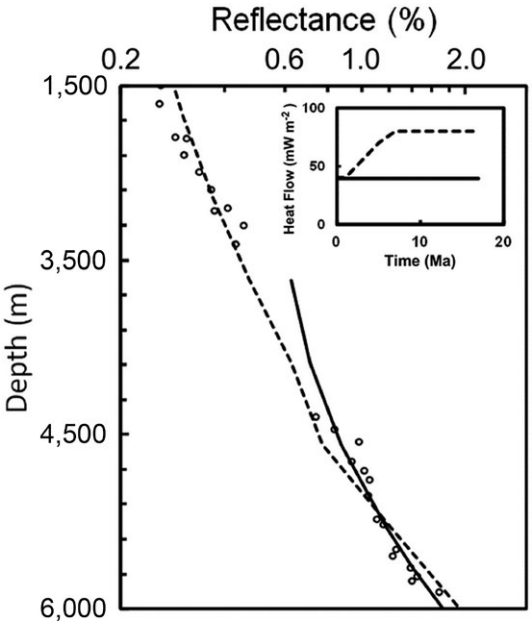


**FIGURE 3** Measured vitrinite profiles from the coast of the Gulf of Mexico and calculated reflectance values from the BDW model (solid line) and the EASY%$R_o$ model (dashed line). Heat flows through time to produce these models are inset. These data are primary vitrinite data from Figure 5 in Dow (1977) which identified that the data are from the Miocene section

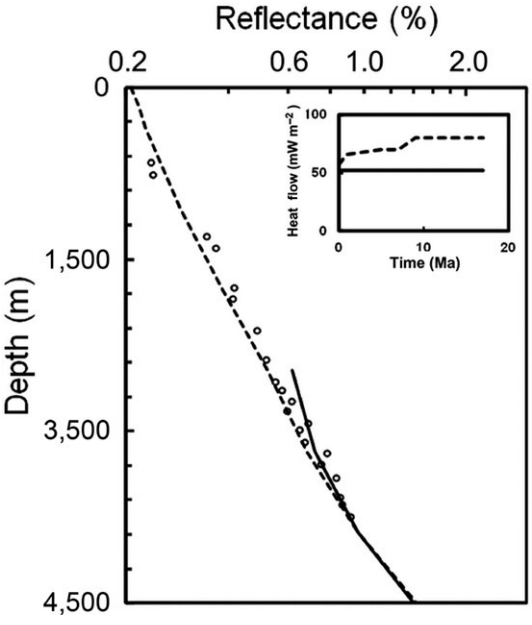


**FIGURE 4** Measured vitrinite profiles from the coast of the Gulf of Mexico and calculated reflectance values from the BDW model (solid line) and the EASY%$R_o$ model (dashed line). Heat flows through time to produce these models are inset. These data are primary vitrinite data from Figure 9 in Dow (1977) which identified that the data are from the Miocene section

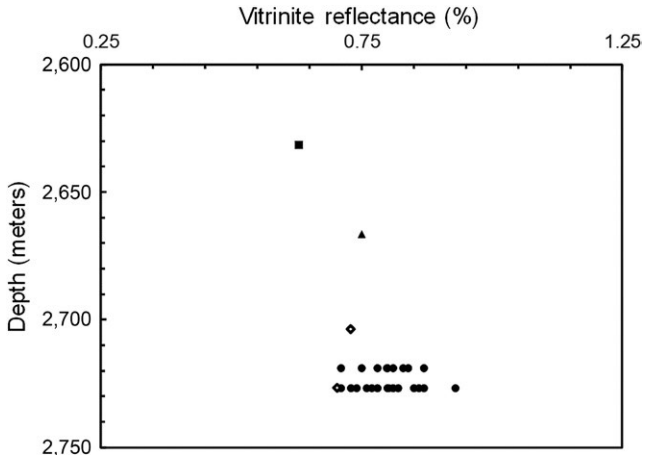


**FIGURE 5** Reported vitrinite data from the DJ Basin. These data are combined from four wells separated by 1 km or less. Each well is denoted with a separate symbol and no supplementary information exists to qualify the reported data. However, it appears that the suite of deeper samples is individual reflectance measurements while the three other wells are individual values which may be an interpreted value from several measurements on one or more samples. Data in these wells are from a very limited depth range, but reported values range from early maturity to late maturity over a vertical distance of less than 200 m. These results may be accounted for by lithological changes or changes in heat flow over short distances (e.g., a fault) and may not necessarily be measurement error

work in this instance, it cannot be guaranteed to work in every application.

## 4 | DISCUSSION

Improving the correlation between measured vitrinite reflectance and calculated reflectance is designed to make vitrinite a more effective tool for establishing physically constrained thermal histories. The EASY%$R_o$ model results in vitrinite reflectance values that are systematically too low. The BDW correlation is better than the EASY%$R_o$ method over the range in vitrinite encountered during hydrocarbon generation and cracking but is not applicable for early maturity ($R_m < 0.56\%$) investigations. Other correlations are possible, and physical and chemical models are encouraged, but in order to be useful the change in calculated vitrinite to the change measured vitrinite, $\frac{dR_c}{dR_m}$, should be close to 1.

In the appendix, it is made clear that Barker (1989) ended their analysis of the reflectance data because the pre-exponential and activation energy calculated from the data set is too low compared to previously published values. It was thought that the low activation energies result in reactions that are too fast and would not properly describe the processes leading to reflectance changes. One of the principal motivations for EASY%$R_o$ is the chemical model on which it is based should provide accurate results; however, the model is systematically too slow and calculated reflectance values are too small. Completing the analysis started by Barker (1989) yields the BDW model which has faster kinetics than the EASY%$R_o$ model and leads to realistic results but over a smaller vitrinite range. The success of the BDW model can be interpreted in a number of ways. First, it can be viewed as a pragmatic model which allows realistic reflectance values to be calculated from thermal models. Second, previously published ranges of realistic activation energies may be broader than thought. Third, a catalytic process affects reflectance that is not sufficiently accounted for in the EASY%$R_o$ model.

An important result of this work is the identification of new methods to extract results from models for calibrating thermal models to vitrinite data. These methods increase the efficiency and understanding associated with calibrating the thermal history of the basin model because they remove the time variable from the calibration process. Placing the model results in the context of a constant age surface shows that only a limited range of vitrinite values is possible in a basin even when complications from uplift and spatially varying heat flows exist.

Determining the portion of a data set to include for calibrating a thermal model is difficult because the set of physically realizable vitrinite values is so limited compared to the range in reported values. However, the general model data shown in Figure 6 are the same for all basins when data are extracted on constant age date surfaces. The range in calculated reflectance is determined by spatial variations in uplift and heat flow. In a margin with constant spatial heat flow and no uplift, the model results are single valued. If the $R_m$ data set is perfect, then the departures between model and data denote variations in uplift or heat flow uncertainty on the maximum temperature. Averaging reflectance measurements in temperature windows leads to good results when sufficient data are present but cannot be guaranteed to be applicable in all cases.

A principle objective of a thermal model calibrated with vitrinite reflectance is the development of physically based estimates for the thermal history of a basin. Physically based means that the thermal conductivity, heat capacity, the surface temperature, and basal heat flow boundary conditions are within bounded ranges. The heat flow model has the form

$$C^v(\phi)\frac{\partial T}{\partial t} = \lambda(\phi)\frac{\partial^2 T}{\partial x_i^2} \tag{2}$$

$$T(x,y,z=0,t) = T_{\text{surface}} \tag{3}$$

$$q(x,y,z=\text{base},t) = q_{\text{basal}} \tag{4}$$

where $C^v$ is the volumetric heat capacity, $T$ is temperature, $t$ is time, $\lambda$ is the thermal conductivity, $x_i$ is the direction, and

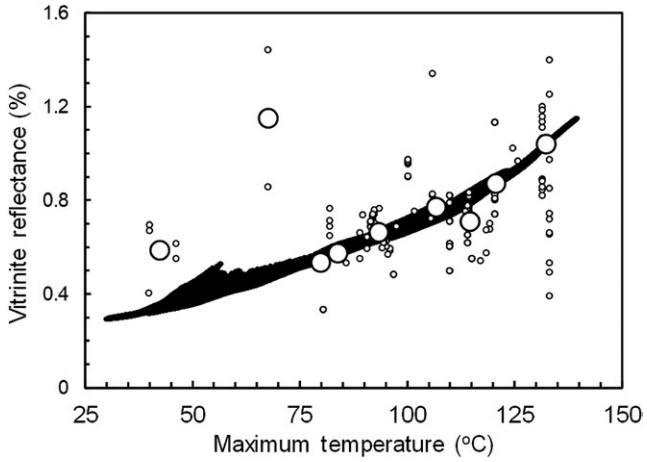


**FIGURE 6** Modelled maximum temperature and calculated vitrinite reflectance are shown on the top of the Niobrara formation in the DJ Basin. Calculated reflectance values, $R_c$, are filled circles and measured vitrinite reflectance data, $R_m$, are open circles. The EASY%$R_o$ model is used for the calculated reflectance. Vitrinite reflectance measurements between the top of the Pierre-Sussex and top of the Fort Hayes Formations are extrapolated to the top Niobrara surface using linear gradients from the basin model. Significant uplift is included in this model and the basal heat flow varies across the basin, so a range in $R_c$ values exists for a single maximum temperature. Measured data exhibit a wide range of values compared to the narrow range of physically realizable values possible for the Niobrara surface. Large open circles are measured vitrinite data and maximum modelled temperatures averaged in 10°C windows starting at 40°C

$\phi$ is the porosity. Boundary conditions at the surface (temperature) and base of the model (heat flow) along with side boundary conditions lead to a unique solution for temperature through time. For the temperature model to be physically bounded then additional requirements are

$$\frac{\phi}{\lambda_f}+\frac{1-\phi}{\lambda_s}<\lambda(\phi)<\lambda_f\phi+\lambda_s(1-\phi) \tag{5}$$

where subscripts $f$ and $s$ describe the thermal conductivity of the fluid and solid. For the heat capacity, a simple series model holds

$$C^v(\phi)=C^v_f\phi+C^v_s(1-\phi) \tag{6}$$

Equations 2–6 are the basis of a well-posed thermal model from which present day temperatures are obtained on a basin scale when the model is populated with regionally consistent lithostratigraphic units for $\lambda$ and $C^v$ (Blackwell & Steele, 1989). A thermal history of the basin is developed using these same equations with sedimentation rates through time and a constitutive relationship, also called a compaction law (Hantschel & Kauerauf, 2009). These thermal histories are the basis for the vitrinite calculations.

The calculated reflectance, $R_c$, is impacted strongly by the present day or maximum temperature. Methods to correct BHT range from robust Horner type methods applied to several temperature measurements (Goutorbe, Lucazeau, & Bonneville, 2007; Horner 1951), to basin scale correlations (Crowell, Ochsner, & Gosnold, 2012) which correct hundreds of BHTs, to multi-basin scale corrections (Blackwell & Richards, 2004; Harrison, Luza, Prater, Cheung, & Ruscetta, 1983) which correct thousands of BHTs. Precision temperature logs (scientific quality measurements accurate and precise to at least 0.1°C) compared to corrected BHTs may be either greater than BHTs (Blackwell & Steele, 1989; McKenna & Blackwell, 2005) or less than these corrected values (Blackwell & Richards, 2004) and the deviations cannot be generalized. Peters and Nelson (2012) suggest that one standard deviation of corrected BHTs is ±8°C which, in their application, leads to an uncertainty in the depth to the oil window of ≈300 m. Figures 1 and 2 show error bars in calculated reflectance due to a 9.3°C uncertainty in present day or maximum temperature at 100°C (2.5% of present day maximum temperature). Most of the calculated reflectance uncertainty is less than 10%. Uncertainty in the depth to the oil window of ≈300 m or less than a 10% uncertainty in calculated values is acceptable, especially given the range of reported measured values in Figure 6.

A best practice to calculate $R_c$ using temperature histories from a basin simulator is to follow the steps in the previous paragraph to calculate the present day thermal model and then estimate the heat flow history through time. Heat flow history should be consistent with major structural events and present day heat flow using data and models from either Blackwell and Richards (2004) or Gosnold (2011). If the basin model from the previous steps accurately captures the sediment type, sedimentation rate, and basin architecture, then adjustments to the heat flow are likely to be consistent with the structural interpretation providing a thermal model that is consistent with the measured and calculated vitrinite reflectance. The key to this consistency is that $\frac{dR_c}{dR_m}=1$.

Uncertainties in measured vitrinite data and calculated reflectance can be significant as shown in Figure 5. However, choosing to extract results on chronostratigraphic surfaces, Figure 6, and base a calibration on average measured values over small temperature windows can lead to an acceptable calibration over a large area. The correspondence between average measured reflectance and the model improves with the number of measurements and increasing maturity. If the average measured reflectance and model are in agreement, then depth estimates to key vitrinite thresholds (e.g., the oil window) should be similar to Peters and Nelson (2012) or ≈300 m.

## 5 | CONCLUSION

We identified a systematic bias with the EASY%$R_o$ method and developed methods to correct these issues with a

transformation of existing EASY%$R_o$ values and a new model (BDW model). A limitation of the BDW model is that it applies over a smaller vitrinite range. Features of the first-order rate equation were identified which make it possible to remove the heating rate dependency of vitrinite reflectance by extracting reflectance data on chronostratigraphic surfaces. This result made clear that data quality in reported vitrinite reflectance measurements allows for multiple interpretations of the thermal history in a basin. Specifically, we conclude:

- EASY%$R_o$ underestimates the measured vitrinite reflectance ($R_m$) by a factor of nearly 2 in a least squares sense for measured vitrinite ranges between 0.2% and 4.7%. This means if vitrinite reflectance is used to constrain a physical thermal model, then the required heat flow to match the data is significantly larger than the actual heat flow required to transform the vitrinite. Model results utilizing vitrinite reflectance as a constraint provide a systematically misleading thermal history of the basin. Although thermal models may appear calibrated, the parameters used to calibrate the model are adjusted in ways that make the model non-physical. In effect, the risk of the prospect or play is passed on to the risk of the model.
- Vitrinite reflectance responds to time and temperature changes and calibrating on a constant age date horizon (e.g., the top Cretaceous) removes the time component of the calibration making it possible to calibrate thermal models to solely maximum temperature. In a margin where there is no uplift and temperature increases monotonically, for each temperature, there is a single physically realizable value of vitrinite reflectance. When uplift occurs, a limited range in reflectance values is possible. Reported measurements outside this range reflect values that are not physically bounded by the chemical kinetic interpretation of the response of vitrinite to temperature changes.
- A large degree of uncertainty exists with vitrinite reflectance measurements reported by different operators in the same basin. We show that extracting these reflectance calculations on chronostratigraphic surfaces and averaging the measured data in small temperature windows (Figure 6) provide acceptable results. The difficulty with this method is every measurement is assumed to have equal validity regardless of sample quality, operator experience, or equipment quality. This result suggests to us that different sampling strategies are required to produce data sets to constrain the thermal history in a basin. One such method may be to focus on measuring a regional marker (e.g., a coal) with a narrow range of stratigraphic ages that is below a common casing point.

## ACKNOWLEDGEMENTS

We thank M. Hertle and S. Ohm and an anonymous reviewer for reading and commenting on the material presented in this paper. Their suggestions improved the content and presentation of this material.

## ORCID

*Tim Matava* https://orcid.org/0000-0001-6676-7552

## REFERENCES

Barker, C. E. (1989). Temperature and time in the thermal maturation of sedimentary organic matter. In N. D. Naesser & T. McCulloch (Eds.), *Thermal history of sedimentary basins* (pp. 73–98). New York, NY: Springer.

Blackwell, D., & Richards, M. (2004). Calibration of the AAPG geothermal survey of North America bht data base. https://www.smu.edu/~/media/Site/Dedman/Academics/Programs/Geothermal

Blackwell, D. D., & Steele, J. L. (1989). Thermal conductivity of sedimentary rocks: Measurement and significance. In N. D. Naesser & T. McCulloch (Eds.), *Thermal history of sedimentary basins* (pp. 13–36). New York, NY: Springer.

Burnham, A. K., & Sweeney, J. J. (1989). A chemical kinetic model of vitrinite maturation and reflectance. *Geochimica et Cosmochimica Acta*, *53*, 2649–2657. https://doi.org/10.1016/0016-7037(89)90136-1

Crowell, A. M., Ochsner, A. T., & Gosnold, W. (2012). Correcting bottom-hole temperatures in the Denver Basin: Colorado and Nebraska. *GRC Transactions*, *36*, 201–206.

Dow, W. G. (1977). Kerogen studies and geological interpretations. *Journal of Geochemical Exploration*, *7*, 79–99. https://doi.org/10.1016/0375-6742(77)90078-4

Fang, H., & Jianyu, C. (1992). The cause and mechanism of vitrinite reflectance anomalies. *Journal of Petroleum Geology*, *15*, 419–434. https://doi.org/10.1111/j.1747-5457.1992.tb01043.x

Fleisher, R. L., & Lane, H. R. (1999). Treatise of petroleum geology/handbook of petroleum geology: Exploring for oil and gas traps. Chapter 17: Applied paleontology: AAPG Bulletin.

Galton, F. (1907). Vox populi (the wisdom of crowds). *Nature*, *75*, 450–451. https://doi.org/10.1038/075450a0

Goodarzi, F., & Murchison, D. G. (1973). Oxidized vitrinites – their aromaticity, optical properties and possible detection. *Fuel*, *52*, 90–92. https://doi.org/10.1016/0016-2361(73)90027-6

Gosnold, W. (2011). The global heat flow database of the international heat flow commission. http://www.heatflow.und.edu/index2.html

Goutorbe, B., Lucazeau, F., & Bonneville, A. (2007). Comparison of several bht correction methods: A case study on an Australian data set. *Geophysical Journal International*, *170*, 913–922. https://doi.org/10.1111/j.1365-246X.2007.03403.x

Hackley, P. C., Araujo, C. V., Borrego, A. G., Bouzinos, A., Cardott, B. J., Cook, A. C., … Goncalves, P. A. (2015). Standardization of reflectance measurements in dispersed organic matter: Results of an exercise to improve interlaboratory agreement. *Marine and Petroleum Geology*, *59*, 22–34. https://doi.org/10.1016/j.marpetgeo.2014.07.015

Hackley, P. C., & Cardott, B. J. (2016). Application of organic petrography in North American shale petroleum systems: A review. *International Journal of Coal Geology*, *163*, 8–51. https://doi.org/10.1016/j.coal.2016.06.010

Hantschel, T., & Kauerauf, A. I. (2009). *Fundamentals of basin and petroleum systems modeling* (p. 476). Berlin, Germany: Springer Science & Business Media.

Harrison, W. E., Luza, K. V., Prater, M. L., Cheung, P. K., & Ruscetta, C. (1983). *Geothermal resource assessment in Oklahoma*. Technical Report. Norman, OK: Oklahoma Geological Survey (Special Publication 83-1).

Horner, D. E. (1951). Pressure build-up in wells. *In Proceedings of the third world oil congress*, *world petroleum congress*, The Hague, pp. 25–43.

Jarvie, D. M., Hill, R. J., & Pollastro, R. M. (2005). Assessment of the gas potential and yields from shales: The Barnett Shale model. *Oklahoma Geological Survey Circular*, *110*, 37–50.

Kalkreuth, W., Sherwood, N., Cioccari, G., da Silva, Z. C., Silva, M., Zhong, N., & Zufa, L. (2004). The application of famm (fluorescence alteration of multiple macerals) analyses for evaluating rank of Paraná Basin Coals, Brazil. *International Journal of Coal Geology*, *57*, 167–185. https://doi.org/10.1016/j.coal.2003.12.001

Katz, B., Pheifer, R., & Schunk, D. (1988). Interpretation of discontinuous vitrinite reflectance profiles. *AAPG Bulletin*, *72*, 926–931.

Malinconico, M. L. (2000). Using reflectance crossplots and rotational polarization for determining first-cycle vitrinite for maturation studies. *International Journal of Coal Geology*, *43*, 105–120. https://doi.org/10.1016/S0166-5162(99)00056-7

McKenna, J., & Blackwell, D. (2005). 3-d multiphysics modeling of a producing hydrocarbon field. http://www.dtic.mil/dtic/tr/fulltext/u2/a592620.pdf (Proceedings of the COMSOL Multiphysics Users Conference).

Mukhopadhyay, P. K. (2014). *The implication of maturation and heat flow analysis for conventional (deepwater) and unconventional (shale oil and shale gas) petroleum systems: Evolution through the last 50 years*. Dallas, TX: AAPG Annual Meeting, paper, 87616.

Peters, K. E., & Nelson, P. H. (2012). Criteria to determine borehole formation temperatures for calibration of basin and petroleum system models. *SEPM Special Publication*, *103*, 5–15.

Poole, F. G., & Claypool, R. E. (1984). Petroleum source-rock potential and crude-oil correlation in the great basin. In J. Woodward, F. F. Meisner, & J. L. Clayton (Eds.), *Hydrocarbon source rocks of the greater Rocky Mountain region* (pp. 179–229). Denver, CO: Rocky Mountain Association of Geologists.

Price, L. C., & Barker, C. E. (1985). Suppression of vitrinite reflectance in amorphous rich kerogen–a major unrecognized problem. *Journal of Petroleum Geology*, *8*, 59–84. https://doi.org/10.1111/j.1747-5457.1985.tb00191.x

Rejebian, V. A., Harris, A. G., & Huebner, J. S. (1987). Conodont color and textural alteration: An index to regional metamorphism, contact metamorphism, and hydrothermal alteration. *Geological Society of America Bulletin*, *99*, 471–479. https://doi.org/10.1130/0016-7606(1987)99%3c471:CCATAA%3e2.0.CO;2

Sweeney, J. J., & Burnham, A. K. (1990). Evaluation of a simple model of vitrinite reflectance based on chemical kinetics (1). *AAPG Bulletin*, *74*, 1559–1570.

Thompson-Rizer, C. L., & Woods, R. A. (1987). Microspectrofluorescence measurements of coals and petroleum source rocks. *International Journal of Coal Geology*, *7*, 85–104. https://doi.org/10.1016/0166-5162(87)90014-0

Tissot, B., & Espitalie, J. (1975). Thermal evolution of organic-matter in sediments-application of a mathematical simulation-petroleum potential of sedimentary basins and reconstructing thermal history of sediments. *Revue De L Institut Francais Du Petrole*, *30*, 743–777. https://doi.org/10.2516/ogst:1975026

Veld, H., Wilkins, R., Xianming, X., & Buckingham, C. (1997). A fluorescence alteration of multiple macerals (famm) study of Netherlands coals with normal and deviating vitrinite reflectance. *Organic Geochemistry*, *26*, 247–255. https://doi.org/10.1016/S0146-6380(96)00156-8

Wilkins, R., Sherwood, N., Faiz, M., Teerman, S., & Buckingham, C. (1997). The application of fluorescence alteration of multiple macerals (famm) for petroleum exploration in SE Asia and Australasia. Proceedings of an International Conference on Petroleum Systems of SE Asia and Australasia, Indonesian Petroleum Association, 923–938.

Wilkins, R. W., Wilmshurst, J. R., Russell, N. J., Hladky, G., Ellacott, M. V., & Bucking-ham, C. (1992). Fluorescence alteration and the suppression of vitrinite reflectance. *Organic Geochemistry*, *18*, 629–640. https://doi.org/10.1016/0146-6380(92)90088-F

Wood, D. A. (1988). Relationships between thermal maturity indices calculated using Arrhenius equation and Lopatin method: Implications for petroleum exploration. *AAPG Bulletin*, *72*, 115–134.

**How to cite this article:** Matava T, Matt V, Flannery J. New insights on measured and calculated vitrinite reflectance. *Basin Res*. 2018;00:1–15. https://doi.org/10.1111/bre.12317

## APPENDIX
## VITRINITE REFLECTANCE CALCULATED FROM TIME–TEMPERATURE MODELS

Increasing temperature through time leads to the transformation of source rock kerogens to fluid hydrocarbons, reflectance changes of vitrinite, and a host of other reactions. These reactions are modelled as first-order kinetic processes between products and reactants. This appendix develops the mathematical equations used to model a suite of parallel reactions and applies these methods to vitrinite reflectance models. The intent of this section is to present all the material required to duplicate the results presented in the text and estimate the uncertainty of the calculated reflectance.

A general first-order reaction where a reactant is consumed has the form

$$\frac{d}{dt}\ln(W_i) = -K_i \tag{A1}$$

where $W_i$ is the mass of the $i$th vitrinite maceral (the reactant), $t$ is time, and $K_i$ is the reaction rate. Depending on the type of model being constructed, the number of components, $i$, ranges from 1, for a bulk or a single component reaction, to $n$ for a complicated model with multiple reactions. The rate terms for first-order reactions are only a function of temperature and a plot of $\ln(K)$ versus $\frac{1}{T}$ is linear. Equation A1 is then modified to the well-known Arrhenius rate equation

$$\frac{dW_i}{dt} = \frac{dW_i}{dT}\frac{dT}{dt} = -W_i A_i \exp\left(-\frac{E_i}{\mathrm{RT}}\right) \tag{A2}$$

where $A$ is the pre-exponential coefficient, $E$ is the activation energy, and $R$ is the gas constant. Setting the heating rate, $H(t) = \frac{dT}{dt}$ gives

$$\frac{dW_i}{dT} = \frac{-W_i A_i}{H(t)} \exp\left(-\frac{E_i}{\mathrm{RT}}\right) \tag{A3}$$

Finally, let $H^j = \frac{dT}{dt}$ describe a piecewise linear heating rate between temperture $j$ and temperture $j-1$ and then integrating Equation A3 over temperature leads to

$$\ln\left(\frac{W_i^j}{W_i^{j-1}}\right) = -\frac{A_i}{H^j}\int_{T^{j-1}}^{T^j} \exp\left(-\frac{E_i}{\mathrm{RT}}\right) dT \tag{A4}$$

Solving Equation A4 in this same piecewise fashion over the temperature history determines the time history of the mass of the reactant.

An interesting and useful result from Equation A4 is that the reaction on a constant age date surface is only a function of temperature and not time. To show this, assume a constant sedimentation rate through time which implies that the heating rate becomes $H(x,y) = \frac{T(x,y)-T_0}{\Delta t}$ where $x$ and $y$ are spatial directions and $T(x, y)$ is the temperature on the time surface. This simplification leads to

$$\ln\left(\frac{W(T)_i}{W(0)_i}\right) = -\frac{A_i \Delta t}{T(x,y)-T_0}\int_{T^{j-1}}^{T^j} \exp\left(-\frac{E_i}{\mathrm{RT}}\right) dT \tag{A5}$$

The right hand side of Equation A5 is only a function of temperature, $T(x, y)$, because $\Delta t$ is constant. This transforms the general relation in Equation A4, from one which depends on time and temperature to a reaction dependent only on temperature. For a chronostratigraphic surface (e.g., the top of Cretaceous) with constant dip and increasing temperature with burial, plotting reflectance versus temperature is a single monotonic curve.

In the general case of several parallel reactions, summing each reaction in Equation A4 leads to an expression for the extent of the reaction, $F$ (also called the transformation ratio in source rock kinetics). The reaction extent has the form

$$F(t) = 1 - \epsilon_i \frac{W(T)_i}{W(0)_i} \tag{A6}$$

where $\epsilon_i$ is the stoichiometric coefficient of each reaction. The extent of reaction is bounded by $0 < F(t) < 1$ and $F(t = 0) = 0$.

Barker (1989) ended the analysis of the data with Figure A1 and Table 1 citing a large number of studies that suggest the activation energy derived from these data is too small by a factor of 4–10. Barker (1989) suggested that the source of this discrepancy is the functional heating time which is in error, although other sources of error could also be present. An alternative view is that the multiple sources from which this data set was compiled could not all conveniently be controlled by the same systematic error. Furthermore, these data are exactly the same type of data sets used to estimate maturity in hydrocarbon exploration settings. If these data are fundamentally flawed, then the entire methodology to estimate reflectance from temperature histories is in error.

Calculating a numerical reflectance with Equations A4 and A6 requires values for the pre-exponential and activation energy. Figure A1 (Table 1) is rate data from Barker (1989) plotted with the inverse of absolute temperature. The slope of this curve is the ratio of the activation energy to the gas constant which implies an activation energy of 9.0989 kcal/mol and the intercept corresponds to a pre-exponential value of 5111.1 $\mathrm{Ma}^{-1}$.

An additional relationship is required to calculate the reflectance from the extent of the reaction. Figure A2 shows a correlative model of reaction extent with measured reflectance (Barker, 1989). This relationship was presented by Tissot and Espitalie (1975). In practice, geohistories are used to calculate the extent of the reaction, $F$, using Equation A4 (or Equation A5 on a surface of a known age). Calculated reflectance values are then obtained with the correlation in Figure A2

$$R_c = 0.5572 \exp(2.2297F) = \exp(-0.5848 + 2.2297F) \tag{A7}$$

In contrast to bulk analysis of the Barker (1989) data set, the EASY%$R_o$ algorithm (Sweeney & Burnham, 1990) is based on a chemical model which describes the change in reflectance with temperature and time. EASY%$R_o$ utilizes 20 parallel reactions each with different activation energies; however, there is only a single pre-exponential for these reactions. Similar to the correlations used in the Barker (1989) data to calculate vitrinite reflectance, the EASY%$R_o$ model also uses correlations; however, these correlations are between elemental composition and vitrinite reflectance (Sweeney & Burnham, 1990). Calculating reflectance from time–temperature history also uses Equations A4 and A6. Results of the EASY%$R_o$ algorithm applied to the maximum temperature, and functional heating data in Table 1 are shown in the last column in Table 1 and in Figure 2.

## UNCERTAINTY ESTIMATES OF VITRINITE CALCULATIONS

Estimates of the bulk activation energy and pre-exponential terms (Equation A4) from the Barker (1989) data set consists of the uncertainty of the least squares method and the uncertainty

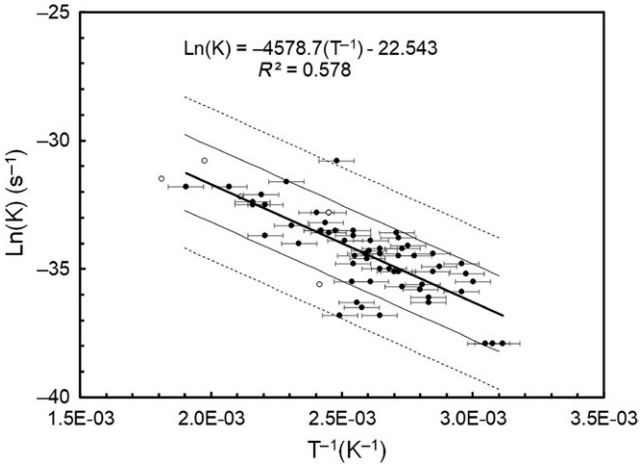


**FIGURE A1** Natural logarithm of reaction rate and inverse absolute temperature for the reflectance data in Table 5.2 (Barker, 1989) and Table 1 of this text. Rate parameters are determined from the slope and intercept of the least squares approximation. We refer to reflectance values calculated with a model based on these data as the BDW model which is a bulk model. The narrow error bands (thin solid line) are the from the standard error of the least squares model (1.48) while the dashed lines are for two times the standard error of the model. Error bars on the data assume a 2.5% uncertainty in the absolute temperature. Open circles denote data that were beyond the error bands in Figure 1 and are not used in the least squares approximation. These data are shown in bold at the bottom of Table 1

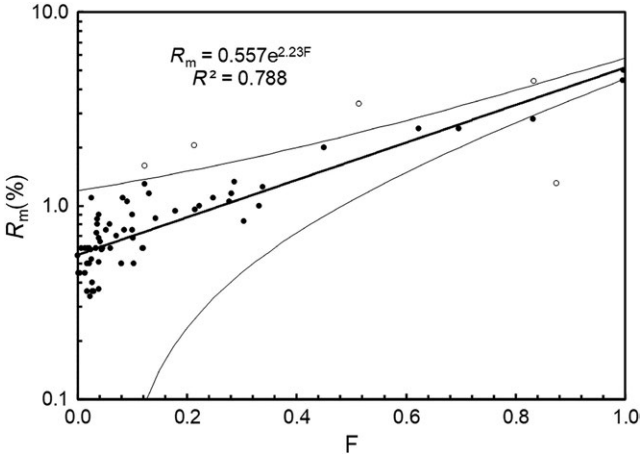


**FIGURE A2** Reaction extent and measured vitrinite data using the Barker (1989) data set. These data show significant uncertainty early in the reaction (small $F$) and show that the applicability is limited to measured values of reflectance that are >0.56%. Error bands are from the standard error of the model which is 0.637. Open circles denote data from Figure 1 that extend beyond the error bands. These data are not used in the least squares approximation. These data are shown in bold at the bottom of Table 1

in present day or maximum temperature. In this section, we address these two uncertainties on the overall quality of the numerical vitrinite calculation.

Figure 1 shows the least squares fit of calculated reflectance values to measured values. The two bounding curves are the standard error of the estimate which is 0.482. Based on the error bands, five data points in Table 1 are excluded from the analysis. These excluded data are shown as open circles in Figures 1, A1, and A2.

Figure 2 shows a least squares fit to measured reflectance values using the EASY%$R_o$ method. The standard error of the estimate is 0.600. Only one data point extends slightly beyond the standard error curve and it is included in the analysis.

The objective of forward modelling vitrinite values is to estimate the time–temperature history as it pertains to the maturity history of source rocks. The time–temperature history is affected by thermal boundary conditions, basin architecture, sediment type, and sedimentation rate all of which can be investigated with an integrated basin simulator. In these models, a particular temperature history is a scenario, based on the geologic model, that should be constrained by the Equations 2–6 so that the thermal modelling is developed using specific heat and thermal conductivity values that are bounded. Multiple geologic scenarios become important to obtain ranges of possible physically bounded temperature histories, but scenarios do not provide estimates of uncertainty of the calculations.

The Barker (1989) data set consists of present day temperature and heating duration which are used to calculate vitrinite reflectance assuming a linear heating rate. Time is usually well constrained with biostratigrahic data but can also be a source of uncertainty. Present day temperature uncertainty, however, is well known and even a corrected bottom hole temperature may have significant uncertainty. We estimate the impact of time–temperature uncertainty on the vitrinite calculations by propagating temperature uncertainties into the vitrinite calculation.

Assume that the uncertainty on the vitrinite calculation is both a function of temperature and time, then the uncertainty in the calculated reflectance is

$$\delta R_c = \frac{\partial R_c}{\partial T}\delta T + \frac{\partial R_c}{\partial t}\delta t \tag{A8}$$

where $\delta T, \delta t$ and $\delta R_c$ are estimates of the temperature, time, and calculated reflectance uncertainties. Substituting Equation A7 into the right hand side of Equation A8 leads to an expression for the change in calculated reflectance in terms of the reaction extent. This new equation is rewritten as

$$\frac{\delta R_c}{R_c} = b\left(\frac{\partial F}{\partial T}\delta T + \frac{\partial F}{\partial t}\delta t\right) \tag{A9}$$

Equation A6 substituted into Equation A9 leads to an expression for the fractional change in calculated reflectance in

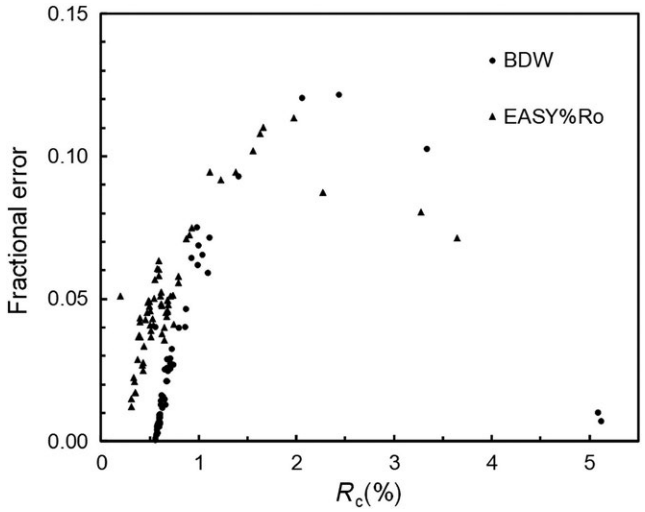


**FIGURE A3** The fractional error in the calculated reflectance plotted against calculated reflectance. The fractional reflectance, $\frac{\delta R_c}{R_c}$, is based on a 2.5% present day temperature uncertainty (±9.3°C at 100°C) and is calculated using Equation A10. In most oil and gas situations, uncertainty of the calculated reflectance is less than 10%

terms of component masses. Arranging the right hand side to obtain the same form as the integral equation for component masses gives

$$\frac{\delta R_c}{R_c} = -b\epsilon_i \frac{W(T)_i}{W(0)_i}\left[\frac{\partial}{\partial T}\ln\left(\frac{W(T)_i}{W(0)_i}\right)\delta T + \frac{\partial}{\partial t}\ln\left(\frac{W(T)_i}{W(0)_i}\right)\delta t\right] \quad \text{(A10)}$$

Equation A10 is the calculated reflectance uncertainty due to uncertainties in temperature and time. Each parallel reaction, *i*, is summed to determine the overall effect on the vitrinite calculation. Unfortunately, we have little insight into the time uncertainty in the Barker (1989) data, so we limit ourselves to the temperature part of the uncertainty calculation where ranges in temperature have been quantified. We assume that the corrected temperature uncertainty is 2.5% of the reported temperature or ±9.3°C at 100°C. Peters and Nelson (2012) suggest that one standard deviation of corrected BHTs is ±8°C.

Results of propagating the temperature uncertainty into the vitrinite reflectance calculation using Equation A10 are shown in Table 1 and Figure A3. At low calculated reflectance values (<1%), the temperature uncertainty leads to a <5% uncertainty in calculated reflectance. At these low calculated reflectance values, the EASY%$R_o$ model has more uncertainty than the BDW model. At calculated reflectance values near 2%, both models have a calculated reflectance uncertainty which ranges from 10 to 15%. For calculated reflectance values between 2% and 4%, the calculated uncertainty in reflectance decreases with increasing reflectance and is generally less than 10%. In these cases, the BDW model exhibits more uncertainty than the EASY%$R_o$ model.

In the body of the paper, it was concluded that the main source of interpretation uncertainty in Figure 6 is the large range of reported measured vitrinite values which are approximately 2–5 times the range of uncertainty in calculated reflectance values. This conclusion still holds: the main source of interpretation uncertainty is the vitrinite measurement. Supporting this interpretation is the observation that the range in reported measured reflectance in Figure 6 is not significantly different from the range in measurements reported in round robin tests amongst different operators (Hackley et al., 2015).